Edelweiss Applied Science and Technology
ISSN: 2576-8484
Vol. 9, No. 10, 223-230
2025
Publisher: Learning Gate
DOI: 10.55214/2576-8484.v9i10.10385

Study of acoustic emission under cyclic loading of dissimilar welded joints of 12kh18n10t and grade 20 steel

V.A. Barat[1,2*], A.Yu. Marchenkov[1], A.Yu. Poroykov[1], E.A. Lepsheev[1,2], A.A. Pankina[1], N.V. Lavrik[1]
[1]Moscow Power Engineering Institute, 111250, Moscow, Krasnokazarmennaya st. 17, Russia; Vera.barat@mail.ru (V.A.B.), art-marchenkov@yandex.ru (A.Yu.M.), Poroykovay@gmail.com (A.Y.P.), LepsheevYA@mpei.ru (E.A.L.) LavrikNV@mpei.ru (N.V.L.)
[2]LLC "INTERUNIS-IT", 111024, Moscow, Shosse Entuziastov st, 20B, Russia.

Abstract: The paper is devoted to the study of acoustic emission (AE) under cyclic loading of dissimilar welded joints. The object of the study is carbide and decarburized diffusion interlayers that are formed during the welding of pearlitic and austenitic steels, as well as during the subsequent operation of such dissimilar joints under high temperatures. The paper presents the results of an experimental study on cyclic loading of samples of dissimilar welded joints with the registration of AE data and measurement of local deformation fields using the digital image correlation (DIC) method. Loading was carried out in the elastic region at a stress close to the operational values. Analysis of the deformation distribution fields over the surface of the samples showed that welded joints with diffusion interlayers have increased deformation values in the interlayer zone. According to the values of the AE parameters, the level of activity and amplitudes of AE hits for samples with diffusion interlayers are higher than in defect-free samples.

Keywords: *Acoustic emission, Diffusion interlayers, Dissimilar welds.*

1. Introduction

Among the modern methods that allow observing the dynamics of the development of physical processes associated with metal deformation, AE occupies a special place due to its high sensitivity to elementary sources associated with the movement of dislocations, twinning, or phase transformations [1]. Different sources correspond to different forms and frequency spectra of AE signals; therefore, the use of the AE method allows us to find out the mechanisms of material deformation, determine the stages of its destruction, and predict damage to the material under variable or mixed types of loading.

Thus, when studying the mechanism of deformation of magnesium alloys in papers [2, 3], differences in the predominance of twinning and dislocation slip processes for fine-grained and coarse-grained materials were revealed based on the energy and spectral parameters of AE signals. In intermetallic alloys [4], as well as in TRIP/TWIP steels [5], which have shape memory, the AE method allows identifying the stages of martensitic phase transformations. Using AE data, it is also possible to analyze the stress-strain state of the material under various or mixed types of loading [6, 7] and predict the moment of failure of the structure [8].

One of the current applications of the AE method is the study of the deformation of additive-manufactured metals. In the process of additive manufacturing, the material of each layer is repeatedly subjected to complex thermal cycles consisting of remelting, heating, and cooling, which affect the parameters of the microstructure of the deposited material. The use of the AE method allows us to

History: Received: 20 August 2025; Revised: 22 September 2025; Accepted: 26 September 2025; Published: 7 October 2025
* Correspondence: Vera.barat@mail.ru

clarify the mechanisms of deformation of deposited materials. The study of the AE features during the deformation of stainless steels obtained by additive manufacturing is presented in Chen et al. [9].

In addition to materials with a complex deformation mechanism, the use of AE is also relevant for studying complex-structured materials, such as concrete, reinforced concrete, and composite materials. The deformation and destruction of each structural element are accompanied by the generation of AE signals with specific parameters of waveform and frequency spectrum [10-12]. Analysis and classification of AE data allow us to identify and separate processes associated with the destruction of various elements and to determine the stages of material destruction.

The object of study in this paper is dissimilar welded joints of pearlitic and austenitic steels, which are objects with a complex microstructure caused by both the difference in the thermal and mechanical properties of the welded steels and the possible formation of diffusion carbide and decarburized interlayers in the fusion zone. The interlayers are usually small in size, but their presence can critically affect the strength properties of the welded joint by reducing its service life and the values of the maximum permissible mechanical stresses.

There are a few works confirming the possibility of detecting defects in dissimilar welded joints using the AE method. In the paper by Barat et al. [13], it is shown that diffusion layers are a source of AE and can be detected during static tension of samples of dissimilar welded joints. In research, Barat et al. [14] revealed differences in the waveform of signals obtained during the deformation of dissimilar welded joints with diffusion interlayers are observed.

This work is a development of works [13, 14] and considers dissimilar welded joints of steel grade 20 (carbon steel with a ferritic–pearlitic microstructure) and 12Kh18N10T steel (austenitic steel), the most common in industry. The aim of the study was to investigate the features of deformation of dissimilar welded joints under cyclic loading and to determine the principles of detection of diffusion interlayers by the AE method.

2. Materials and Methods of the Research

Dissimilar welded joints of steel 20 and steel 12Kh18N10T were considered the objects of the current research. To manufacture welded joints, sheets of these steels, 3 mm thick, were used. The sheets were cut into strips 1000 mm long and 200 mm wide and welded together using tungsten inert gas welding (TIG).

TIG carried out butt-welding on both sides; the filler material chosen was Sabaros O101 wire (Table 1). The use of Sabaros O101 wire allows, on the one hand, to obtain an austenitic microstructure of the weld metal; on the other hand, the chromium content in the wire contributes to the formation of carbide and decarburized diffusion interlayers during heat treatment of welded joints.

Table 1.
Chemical composition of Sabaros O101 filler wire for TIG, % by weight.

C	Si	Cr	Ni	Mn	Fe
0.10	0.50	19.0	9.0	6.0	base

Some of the plates were subjected to heat treatment simulating long-term operation of welded joints at high temperatures, which led to the formation of diffusion interlayers in the welded joints. Heat treatment was performed in a Nabertherm P180 furnace at a temperature of 650°C. To form interlayers of different thicknesses, heat treatment was carried out with different holding times (for 1 hour, 5 hours, 50 hours). The average values of the thicknesses of the diffusion interlayers are shown in Table 2.

Edelweiss Applied Science and Technology
ISSN: 2576-8484
Vol. 9, No. 10: 223-230, 2025
DOI: 10.55214/2576-8484.v9i10.10385

Table 2.
Average values of diffusion interlayer thickness after heat treatment.

Mode No.	Holding Time, hrs	Decarburized interlayer thickness, µm	Carbide interlayer thickness, µm
1	1	145	20
2	5	225	45
3	50	600	65

An increase in the holding time and heat treatment temperature leads to an intensification of the process of carbon diffusion from steel 20 into the weld metal, resulting in an increase in the thickness of the decarburized and carbide interlayers (Figure 1).

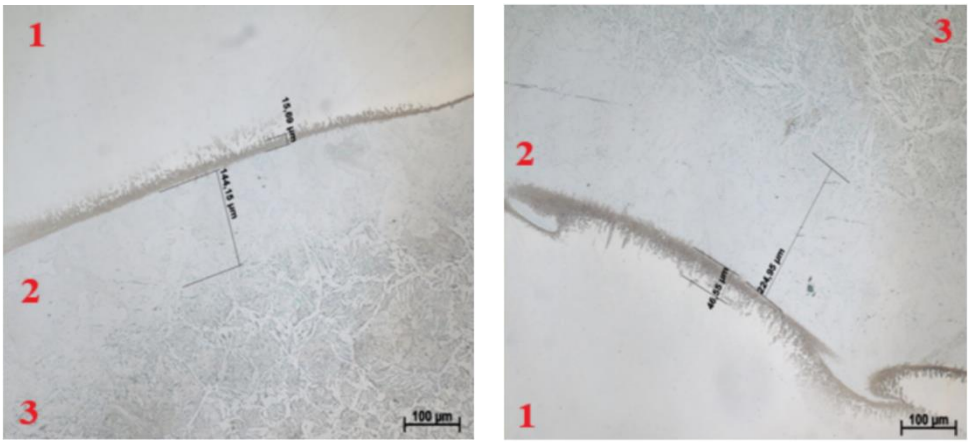

a. b.

Figure 1.
Photographs of the fusion line from the side of steel 20 with measured values of diffusion interlayer thickness after heat treatment at 650°C with a holding time of 1 hour (a), 5 hours (b).

Samples for mechanical testing were manufactured using laser cutting. The drawing of the sample is shown in Figure 2b. Samples of dissimilar welded joints were tested for cyclic tension with synchronous recording of AE data and measurement of local deformation by the DIC method. The tests were carried out on an Instron 5982 machine with triangular pulsation cycles at a maximum tensile stress of 200 MPa with a frequency of 0.15 Hz. The loading diagram is shown in Figure 2c.

Edelweiss Applied Science and Technology
ISSN: 2576-8484
Vol. 9, No. 10: 223-230, 2025
DOI: 10.55214/2576-8484.v9i10.10385

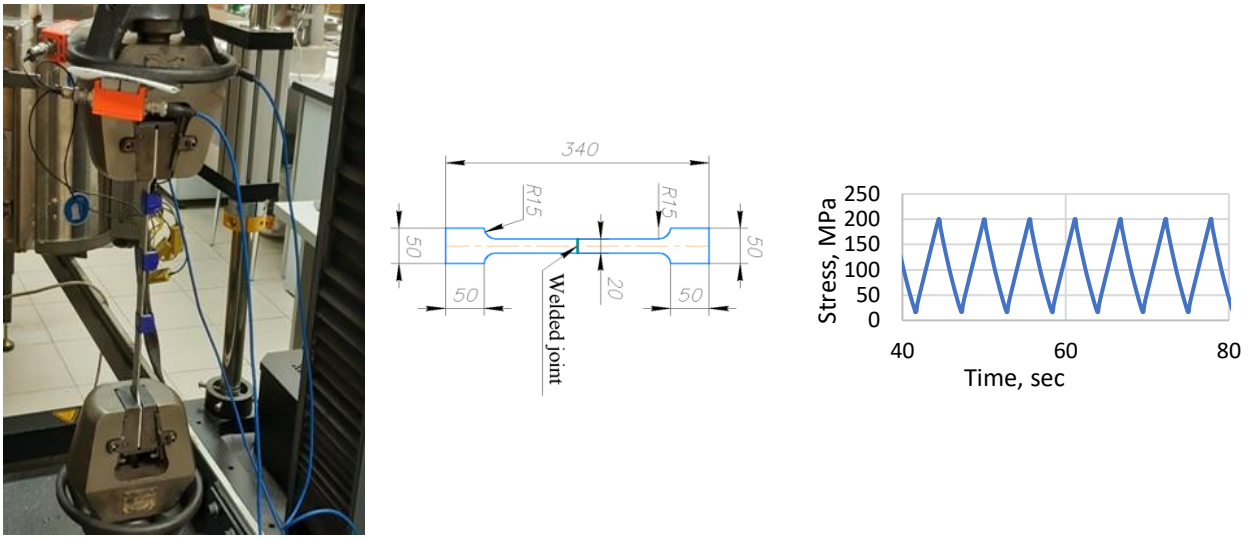

a. b. c.

Figure 2.
Photograph of a sample in grips with fixed AE sensors (a), drawing of the sample with a weld joint (b) and loading diagram (c).

The AE data were recorded using the A-Line 32D system (Interunis-IT LLC) with PAEF-014 preamplifiers and GT200 AE sensors (Global Test LLC) with a resonant frequency of 180 kHz. To suppress the noise of the test machine during data collection, a digital filter with a passband of 100-400 kHz, shifted to the high-frequency region, was used. The amplitude discrimination threshold was set at 32 dB.

To measure the strain fields during specimen loading, a DIC method was used based on a LaVision measuring system with two monochrome CCD cameras (resolution 2456×2058 pixels, matrix size 2/3 inch). In each experiment, the displacement fields were recorded at a frequency of 1 frame per second and saved as 12-bit images with a size of 2300×1200 pixels, which corresponds to a specimen area of approximately 100×20 mm. The displacement distribution was recorded during the test, and then the measured displacement distribution was used to calculate the strain maps.

3. Results

The tensile stress-strain diagrams of dissimilar welded joint samples (Figure 3) have several characteristic sections. For a welded sample without heat treatment (Diagram 1), up to a stress of about 250 MPa, which corresponds to the yield strength of 12Kh18N10T steel, both steels and the weld metal are elastically deformed. At a stress of approximately 250 MPa, plastic deformation of 12Kh18N10T steel begins, and at around 320 MPa, a yield plateau from steel 20 is observed. The yield plateau is followed by a developed section of strain hardening, in which both steels are plastically deformed. The tensile stress diagrams of welded samples after various heat treatment modes are shown in Figure 3 (Diagrams 2–3). It is evident from the diagrams that during heat treatment, the strength characteristics of the welded samples remained at the same level.

Edelweiss Applied Science and Technology
ISSN: 2576-8484
Vol. 9, No. 10: 223-230, 2025
DOI: 10.55214/2576-8484.v9i10.10385

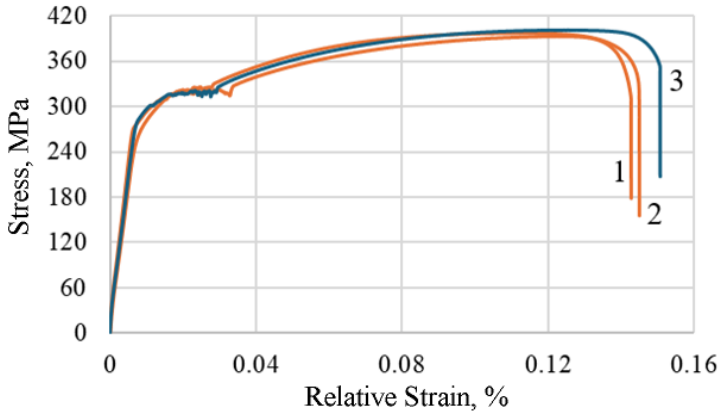

Figure 3.
Tensile diagrams of dissimilar welded joint samples of 20 and 12Kh18N10T steels with stress, MPa, and relative elongation, % respectively (1 – without heat treatment, 2 – 1 hour, 650°C, 3 – 5 hours, 650°C).

However, when measuring the strain fields during cyclic loading of samples, features associated with the presence of diffusion layers were revealed. Figure 4 shows the distributions of the normal component of deformation in the weld seam area and the heat-affected zone of the welded joint for the time moment corresponding to the maximum cycle stress of σ_{max}=200 MPa.

In the experiment with a defect-free sample, the deformation is predominantly uniform (Figure 4a). In the presence of diffusion interlayers, the distribution of strain becomes asymmetric due to the appearance of an area with an increased strain level in the near-weld zone on the side of steel 20. Figure 4b shows the distribution of strain at a maximum cycle stress of 200 MPa for a sample of a dissimilar welded joint with a decarburized diffusion interlayer of about 225 μm. The strain level in the area of the diffusion interlayer is, on average, about 0.008 (0.8%), which significantly exceeds the strain level in other areas of the welded joint sample.

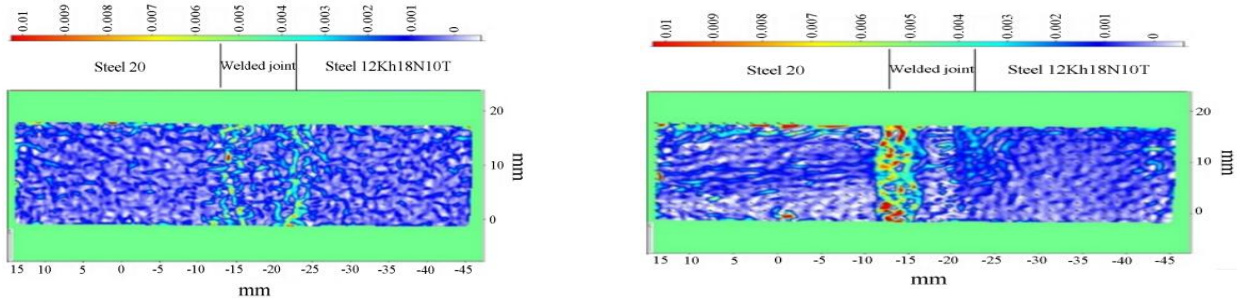

Figure 4.
Fields of local deformations measured by the DIC method for a defect-free sample (a) and for a sample with a 225 μm decarburized diffusion interlayer (b).

From the point of view of AE data, cyclic loading of samples is a stationary process with a constant level of AE activity. Figures 5a and 5c show the AE hits rate for three samples of dissimilar welded joints: a sample without diffusion interlayers and with diffusion interlayers of 145 and 225 μm thickness. In all experiments, the AE hits rate was quite low, since the nature of loading of the samples corresponded mainly to the region of elastic deformation. The average value of activity in the test series

Edelweiss Applied Science and Technology
ISSN: 2576-8484
Vol. 9, No. 10: 223-230, 2025
DOI: 10.55214/2576-8484.v9i10.10385

changed insignificantly, in the range from 0.12 to 0.22 hits per second, with a tendency to increase with an increase in the thickness of the diffusion interlayer.

Compared with the AE hit rate, amplitude parameters are more informative. Figure 5d - 5f shows different distributions of AE hit amplitudes for defect-free samples and samples with diffusion interlayers of different thicknesses. The distribution of AE hit amplitudes for a sample without diffusion interlayers corresponds to an exponential law (determination coefficient $R^2 > 0.92$).

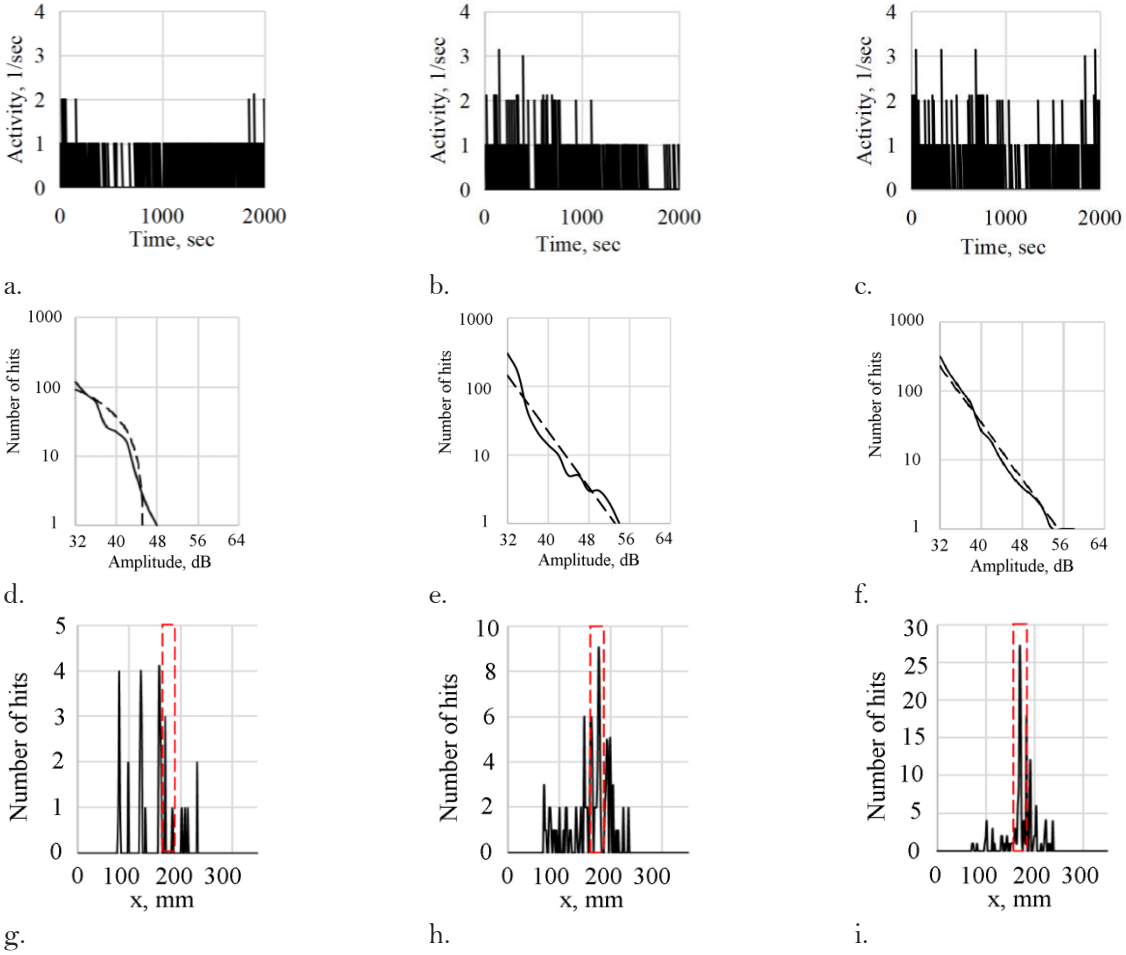

Figure 5.
AE hit rate (a - c), distribution of AE hit amplitudes (d - f), results of linear location (g - i) for a defect-free sample (a, d, g) for a sample with a 145 μm decarburized diffusion interlayer (b, e, h) for a sample with a 225 μm decarburized diffusion interlayer (c, f, i).

For samples with diffusion interlayers, the character of the amplitude distribution changes (Figure 5e, 5f). Figures 5e and 5f show the amplitude distributions for samples with decarburized diffusion interlayer thicknesses of approximately 145 μm and 225 μm, respectively. In these cases, the distribution corresponds to the Gutenberg-Richter law $lgN = a - bA_{dB}$, where A_{dB} is the hit amplitude, and N is the number of hits of a given amplitude ($R^2 > 0.93$).

The most visible result in identifying diffusion interlayers is achieved by locating AE sources. Figure 5i-g shows three graphs containing the location results for samples without diffusion layers and with decarburized diffusion interlayers of 145 and 225 μm thickness. In each of the graphs, the x-axis indicates the distance x from the edge of the sample (the zone from 0 to 165 mm corresponds to

Edelweiss Applied Science and Technology
ISSN: 2576-8484
Vol. 9, No. 10: 223-230, 2025
DOI: 10.55214/2576-8484.v9i10.10385

12Kh18N10T steel, from 160 to 180 mm – to the weld and heat-affected zone, from 180 to 340 mm – to grade 20 steel), and the y-axis shows the number of AE events localized at the point with the coordinate *x*.

Figure 5g corresponds to a defect-free sample. On this graph, the AE event indications are located randomly along the x-axis. The number of localized AE events is small and amounts to 3-5% of the total data volume. Figures 5h and 5i show the location results corresponding to a sample with a diffusion interlayer. The total number of localized events increased and amounted to 15-20%. Additionally, a location cluster is visualized in the weld joint location zone.

4. Conclusions

The paper examines the characteristics of acoustic emission (AE) under cyclic loading of samples from dissimilar welded joints of pearlitic and austenitic steels. The focus of the study was on diffusion-decarburized and carbon interlayers, which are microstructural defects within dissimilar welded joints. Based on the research findings, it was determined that the presence of diffusion interlayers can be detected through an increase in AE pulse amplitudes. The amplitudes of AE hits for defect-free samples did not exceed 48 dB, and their distribution followed an exponential law. In contrast, when diffusion interlayers were present, the amplitude levels increased to between 55 and 60 dB, and the distribution of amplitudes shifted from exponential to power-law behavior.

When testing samples with diffusion interlayers, according to the DIC method, in the area of the fusion line on the side of steel 20, a zone with increased deformation values is detected, the location of which coincides with the location of the decarburized diffusion interlayer, and according to the AE data, a location cluster is determined in the weld joint zone, including up to 30 AE events. The presence of a location cluster is a stable diagnostic feature that allows identifying the presence of diffusion interlayers in the weld joint zone.

Funding:

The work was carried out as part of the project "Development of a methodology for detecting sensitization processes and intergranular corrosion formation in austenitic steels using acoustic emission" (Grant Number: PNI-24/26-34), supported by a grant from the National Research University "Moscow Power Engineering Institute" (NRU "MPEI") for the implementation of the research program "Priority 2030: Technologies of the Future" in 2024–2026.

Transparency:

The authors confirm that the manuscript is an honest, accurate, and transparent account of the study; that no vital features of the study have been omitted; and that any discrepancies from the study as planned have been explained. This study followed all ethical practices during writing.

References

[1] A. Vinogradov, I. Yasnikov, and D. Merson, "Phenomenological approach towards modelling the acoustic emission due to plastic deformation in metals," *Scripta Materialia*, vol. 170, pp. 172-176, 2019. https://doi.org/10.1016/j.scriptamat.2019.06.011

[2] A. Vinogradov, D. Orlov, A. Danyuk, and Y. Estrin, "Effect of grain size on the mechanisms of plastic deformation in wrought Mg–Zn–Zr alloy revealed by acoustic emission measurements," *Acta Materialia*, vol. 61, no. 6, pp. 2044-2056, 2013. https://doi.org/10.1016/j.actamat.2012.12.024

[3] D. Salita and V. Polyakov, "Acoustic emission during plastic deformation of Pb–Sn alloys," *Physical Mesomechanics*, vol. 23, pp. 593-600, 2020. https://doi.org/10.1134/S1029959920060156

[4] Y. N. Vjunenko, V. Kozhushko, A. Volkov, and E. Chernyaeva, "Acoustic emission during the thermal cycling of titanium nickelide under conditions of uneven heating," *Bulletin of the Russian Academy of Sciences: Physics*, vol. 81, pp. 1304-1309, 2017. https://doi.org/10.3103/S106287381711020X

[5] M. Linderov, C. Segel, A. Weidner, H. Biermann, and A. Vinogradov, "Deformation mechanisms in austenitic TRIP/TWIP steels at room and elevated temperature investigated by acoustic emission and scanning electron microscopy," *Materials Science and Engineering: A*, vol. 597, pp. 183-193, 2014. https://doi.org/10.1016/j.msea.2013.12.094

[6] J. Li *et al.*, "Revealing dislocation activity modes during yielding and uniform deformation of low-temperature tempered steel by acoustic emission," *Journal of Iron and Steel Research International*, vol. 31, pp. 3022-3036, 2024. https://doi.org/10.1007/s42243-024-01253-y

[7] L. Botvina, A. Bolotnikov, I. Sinev, and E. Beletsky, "Acoustic emission, damage and fracture mechanisms of structural steel under mixed-mode loading," *Engineering Fracture Mechanics*, vol. 292, p. 109635, 2023. https://doi.org/10.1016/j.engfracmech.2023.109635

[8] K. Barat, H. Bar, D. Mandal, H. Roy, S. Sivaprasad, and S. Tarafder, "Low temperature tensile deformation and acoustic emission signal characteristics of AISI 304LN stainless steel," *Materials Science and Engineering: A*, vol. 597, pp. 37-45, 2014. https://doi.org/10.1016/j.msea.2013.12.067

[9] Y. Chen, B. Gou, X. Xu, X. Ding, J. Sun, and E. K. Salje, "Multibranches of acoustic emission as identifier for deformation mechanisms in additively manufactured 316L stainless steel," *Additive Manufacturing*, vol. 78, p. 103819, 2023. https://doi.org/10.1016/j.addma.2023.103819

[10] Y. G. Matvienko, N. Makhutov, I. Vasil'ev, D. Chernov, V. Ivanov, and S. Elizarov, "Evaluation of the residual strength of composite products based on the structural-phenomenological concept of damage and acoustic emission diagnostics," *Inorganic Materials*, vol. 59, pp. 1504-1514, 2023. https://doi.org/10.1134/S0020168523150098

[11] V. E. Barsuk, L. N. Stepanova, and S. I. Kabanov, "Composite airplane construction acoustic emission testing during static loading," *Kontrol Diagnostika*, pp. 14–19, 2018. https://doi.org/10.14489/td.2018.04.pp.014-019

[12] S. Jiang *et al.*, "Flexural performance and damage mechanisms of stitched composites under different stitch patterns and densities by acoustic emission," *Thin-Walled Structures*, vol. 204, p. 112323, 2024. https://doi.org/10.1016/j.tws.2024.112323

[13] V. Barat, A. Marchenkov, V. Bardakov, D. Zghut, M. Karpova, and S. Elizarov, "Diagnostics of dissimilar weld joints of austenitic to pearlitic steels by acoustic emission," *Journal of The Institution of Engineers (India): Series D*, vol. 104, pp. 531-538, 2023. https://doi.org/10.1007/s40033-022-00409-y

[14] V. Barat *et al.*, "Assessment of the structural state of dissimilar welded joints by the acoustic emission method," *Applied Sciences*, vol. 12, no. 14, p. 7213, 2022. https://doi.org/10.3390/app12147213

Edelweiss Applied Science and Technology
ISSN: 2576-8484
Vol. 9, No. 10: 223-230, 2025
DOI: 10.55214/2576-8484.v9i10.10385